Monte-Carlo simulations for the LUXE experiment and general considerations on the design

G. Sarri, the Queen's University of Belfast

Abstract

The present document provides detailed information on particle tracking and full-scale Monte-Carlo modelling of the LUXE experiment, with particular emphasis to optimising the signal-to-noise ratio at the particle detectors. All simulations have been performed using the Monte-Carlo scattering code FLUKA.

1 General setup

A scaled sketch of the proposed experimental setup is given in Fig. 1.

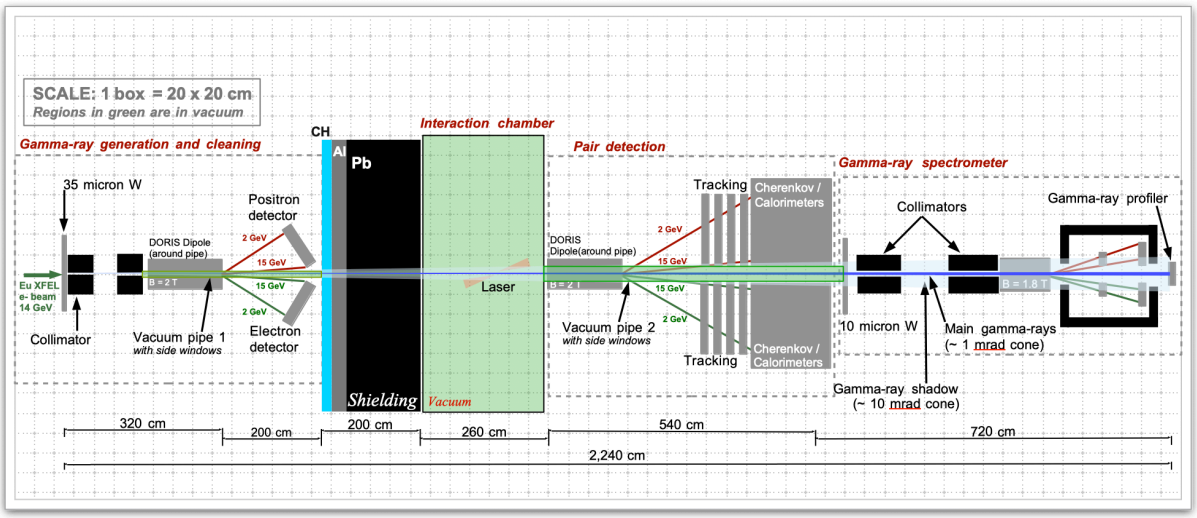

Figure 1: Top-view of the proposed setup. The drawing is in scale, with each square in the grid representing 20 x 20 cm. Regions filled with light green are in vacuum (Pipe1, Interaction chamber, and Pipe 2). The positron trajectories (red), the electron trajectories (green), and the gamma-ray beam (light blue for the overall cone and dark blue for photons with energy exceeding 1 GeV) are also in scale.

The setup assumes realistic values for the magnetic dipoles and an initial electron beam energy of 14 GeV. The setup is easily extendible to the case of 17.5 GeV primary electrons with similar consideration for the signal-to-noise estimates. The electrons will first interact with a 35 micron W target, to generate the primary gamma-ray beam for the experiment. Two cylindrical collimators are then placed after that. The collimators are both 50 cm long, are made of Pb, and are separated by 50 cm. The hole in the first collimator has a diameter of 1 mm and in the second a diameter of 4 mm. The first DORIS magnet (assumed hereafter to work at 2T) is then placed downstream to bend the electrons and positrons onto the beam dump, which is made of 20 cm of CH, 30 cm of Al, and 200 cm of Pb. It is important to have progressively higher atomic numbers in the dump but different materials can be used (i.e., Cu instead of Al) with similar results. The dump has a conical hole (starting with a diameter of 5 cm and ending with a diameter of 10 cm) to minimise interaction of the primary gamma-ray beam with its walls and

the subsequent generation of noise. Between the second collimator and the entrance of the dump there is a vacuum pipe with a diameter of 5 cm with an entrance window made of 100 micron of Be. The Be window induces a small correction to the yield of secondary positrons and electrons of the order of 10^{-4} per primary electron, as shown in Fig. 3.

The hole in the dump is also supposed to be in vacuum. We then have the main interaction chamber with a size of 2.6 m, where the laser will be focussed onto the gamma-ray beam. After that, a second vacuum pipe of 20cm diameter extends for 5.4 m ending with a 100 micron Be window. Around the pipe, the second DORIS magnet (operating at 2 T) will bend the electrons and positrons generated at the interaction point onto a suite of detectors consisting of tracking detectors, Cherenkov detectors, and calorimeters. Both magnets are assumed to operate at 2 T, even though they can be tuned up to 2.2 T. 2T appears to be a reasonable value to allow for best signal-to-noise ratio and to guarantee effective separation of the particles from the main gamma-ray cone. At the end of the second pipe a setup to spectrally and spatially characterise the primary gamma-ray beam is shown. Each pipe will have thin low-Z windows at each side to allow the particles to exit it. Overall, the full extent of the setup is 22.4 m.

2 Beam dump

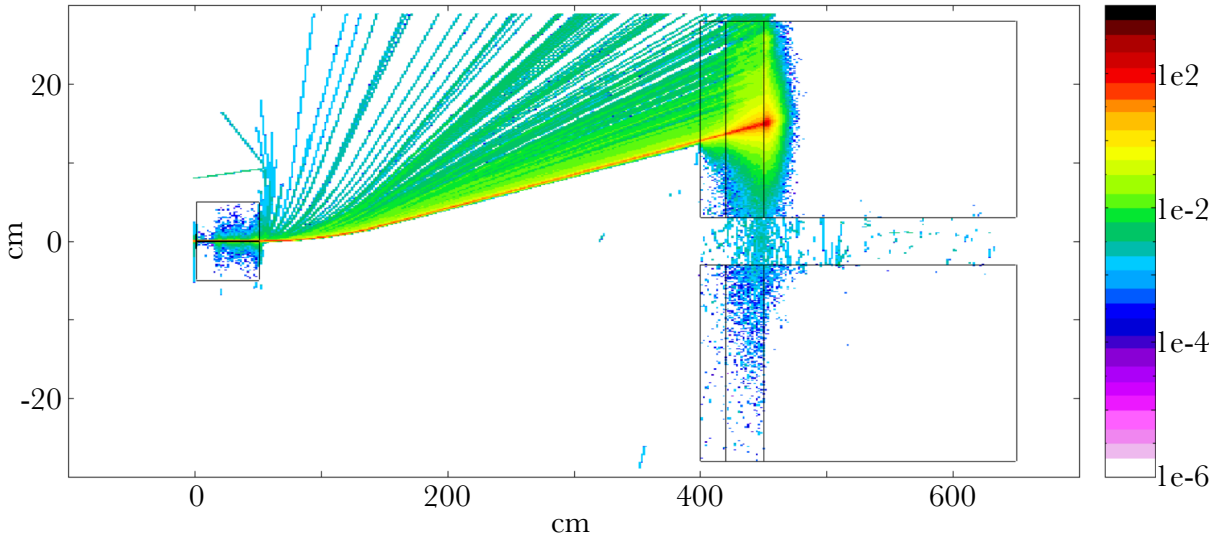

Figure 2: 2-D spatial distribution of the electrons after interaction with the 35 micron W and propagation through the 2T magnet. The beam dump is depicted by the three black rectangles on the right. The spatial scales are in cm on both axis.

The first step is to ensure that the beam dump can effectively kill the primary electron beam after the interaction with the W target. Due to the demanding computation cost of this simulation, only 10^4 primary electrons were assumed in this first simulation. The current design of the beam dump is more than sufficient to stop 6×10^9 electrons at 17.5 GeV and the first magnet operating at 2 T deflects the electrons significantly away from the beam dump aperture. This is shown in Fig. 2, which depicts the simulated electron 2-D spatial distribution. The electrons are deflected upwards, at the entrance of the dump, by at least 12cm, with the hole radius being 2.5 cm. Due to the demanding computation time required to model the beam dump, we will from now on replace it with a fully absorbing body (called black-hole in FLUKA).

3 Full-scale simulations

The full-scale simulations are reported here. For each simulation, we assume a pencil-beam of monoenergetic electrons of 14 GeV. We simulate 10^7 particles per run, due to constraints in computation time ($\approx$ 24 hours per run for the simulations shown here). In Figure 6, the top-view electron, positron, and photon 2D spatial distributions up to the exit of the beam dump are shown.

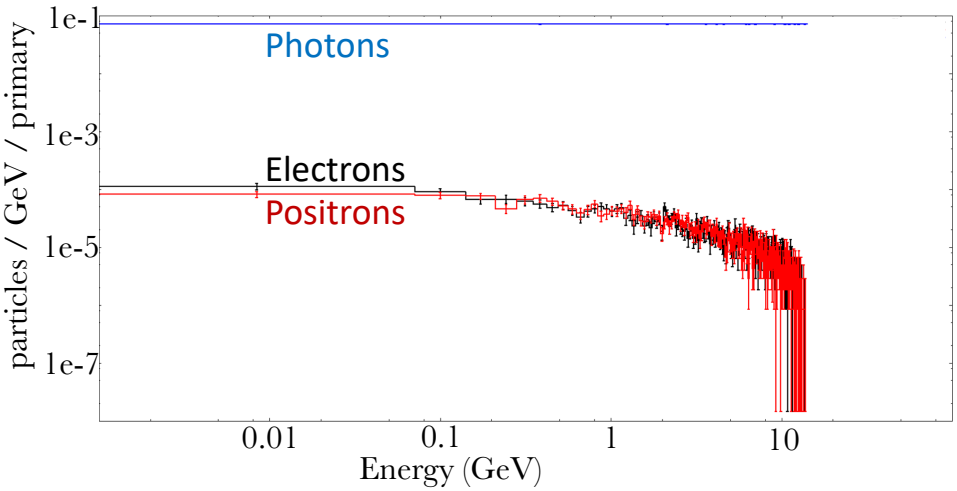

Figure 3: Spectrum of the electrons, positrons, and photons escaping a 100 micron Be slab irradiated by a flat spectrum of gamma-ray photons with a maximum energy of 14 GeV. x-axis represents the particle energies in GeV, whereas the y-axis represents particles per primary per GeV.

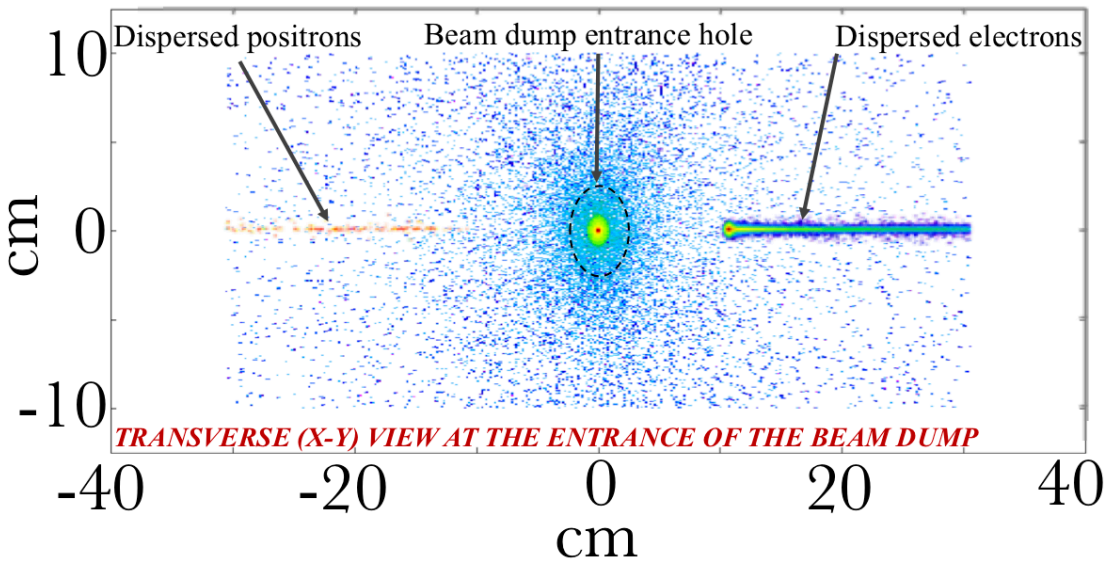

Figure 4: Transverse spatial distribution of the electrons, positrons, and gammas before the beam dump. Spatial scale in cm.

From the figure it is evident that the first two collimators define a clear-cut cone of gamma-rays (full-cone angle of the order of 20 mrad). The hole in the dump is conical, following the divergence of the full gamma-ray beam. All electrons and positrons are effectively deflected away from the main axis and minimal interaction between the inner walls of the dump and the gamma-ray beam is seen. A vacuum pipe with a diameter of 5 cm will be placed between the second collimator and the entrance of the dump. The pipe will have a 100 micron Be window at the entrance, i.e., before the magnet. The Be window will induce a $\approx 10^{-4}$ correction (per primary) to the electron and positron signal (Fig. 3), negligible in this configuration. Approximately 10^{-7} particles per primary are generated inside the beam-dump (close to the resolution of the simulation) but they either do not exit it or they do so at a very broad angle.

In Fig. 4, we show the transverse distribution of the particles before the beam dump (red region in the upper frame). Both electrons and positrons are clearly separated from the main gamma-ray beam. The dispersed positrons are in excess of 10^{-6} per primary per cm^2, while the electrons go approximately from 0.1 per primary per cm^2 (high-end of the spectrum, i.e., closer to the gamma-ray beam) to approximately 10^{-3} per primary per cm^2 (low-end of the spectrum, i.e., further away from the gamma-ray beam). The gamma-ray noise at this plane is below 10^{-6} per primary per cm^2, allowing to detect and spectrally resolve these particles. This is particularly useful as a "control" diagnostic to ensure, on-shot, that the optimum gamma-ray beam was generated.

After the beam dump, the gammas will propagate in two main cones: the high-energy photons (energy > 1 GeV), will propagate with a divergence of 1 mrad, while lower energy photons (as resulting from noise), will propagate with a 20 mrad cone, as set by the hole in the beam dump. At the laser interaction area, no electron tracks and only 8 positron tracks are registered. Given the 10^7 primary particles used in the simulations, this implies that we have a signal to noise better than 10^8 for the electrons and of the order of 1.2×10^6 for the positrons. However, all these single positrons have energies below 1 GeV with no positrons recorded at energies above 1 GeV. These low energy positrons can be easily discerned by the spectrometer and tracking system, implying a signal-to-noise for the positrons above 1 GeV at least of 10^8. Moreover, none of this track are recorded in the central 5x5 cm^2 region, implying that they exit the beam dump at a high angle. Again, this helps the tracking system discarding them.

In the following table, a summary of the main signal and noise at each detector plane (i.e., before the beam dump and after the IP) is given.

	After beam dump			**After interaction point**		
	electron	*positron*	*photon*	*electron*	*positron*	*photon*
Yield signal	0.1 - 10^{-3} per cm^{-2}	$> 10^{-6}$ per cm^{-2}	N/A	3×10^{-8}	3×10^{-8}	0.37
Energy signal	2 - 14 GeV	2 - 14 GeV	N/A	4 - 10 GeV (FWHM)	4 - 10 GeV (FWHM)	1 - 14 GeV
Detector size	30 cm @ 30°	30 cm @ 30°	N/A	80 cm flat	80 cm flat	30 cm flat
Yield noise	N/A	N/A	$< 10^{-6}$ per cm^{-2}	$< 10^{-8}$	8×10^{-7}	$< 10^{-5}$
Energy noise	N/A	N/A	<1 GeV	none detected	< 1 GeV	< 1 GeV
Noise transv. size	N/A	N/A	wide	none detected	outside 5 cm	<15 cm

Table 1: Summary of the main contributions to signal and noise from the Monte-Carlo simulations. The yields are given per primary electron. The table assumes an initial electron energy of 14 GeV. The position of the detectors is shown in Fig. 1. The noise region refers to a radius around central axis. The electron and positron yields at the IP assume 1.5×10^9 primary electrons and $\xi \approx 2.6$

From the table we can see that the detectors before the beam dump should be 30 cm long and tilted by 30 degrees, in order to accept between 2 and 15 GeV. The photon noise at these detectors is orders of magnitude smaller than the electron signal and approximately 10 times smaller than the positron signal, allowing for a clean detection of the particle spectra after the converter. At the interaction point, we can not detect any electrons arising from the noise (i.e., less than 10^{-8} electrons per primary electron) and only 8 positrons. The energy of these positrons is below 1 GeV and none of these traces appear in the central 5×5 cm^{-2} region. No photons from noise are detected outside 15 cm radius from axis. The

transverse distribution of the photons at the interaction point and the single positron tracks are shown in Fig. 5

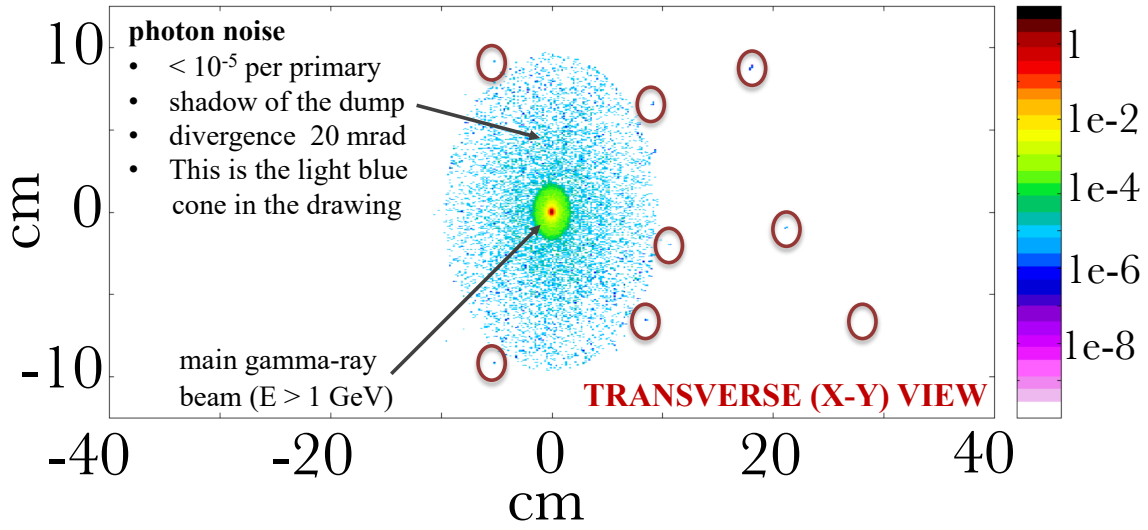

Figure 5: 2-D transverse spatial distribution of the photons at the interaction point. No electrons are detected in this region, and only 8 positron tracks (each with an energy smaller than 1 GeV) are highlighted with red circles. The colourbar is in photons per primary per cm^{-2}

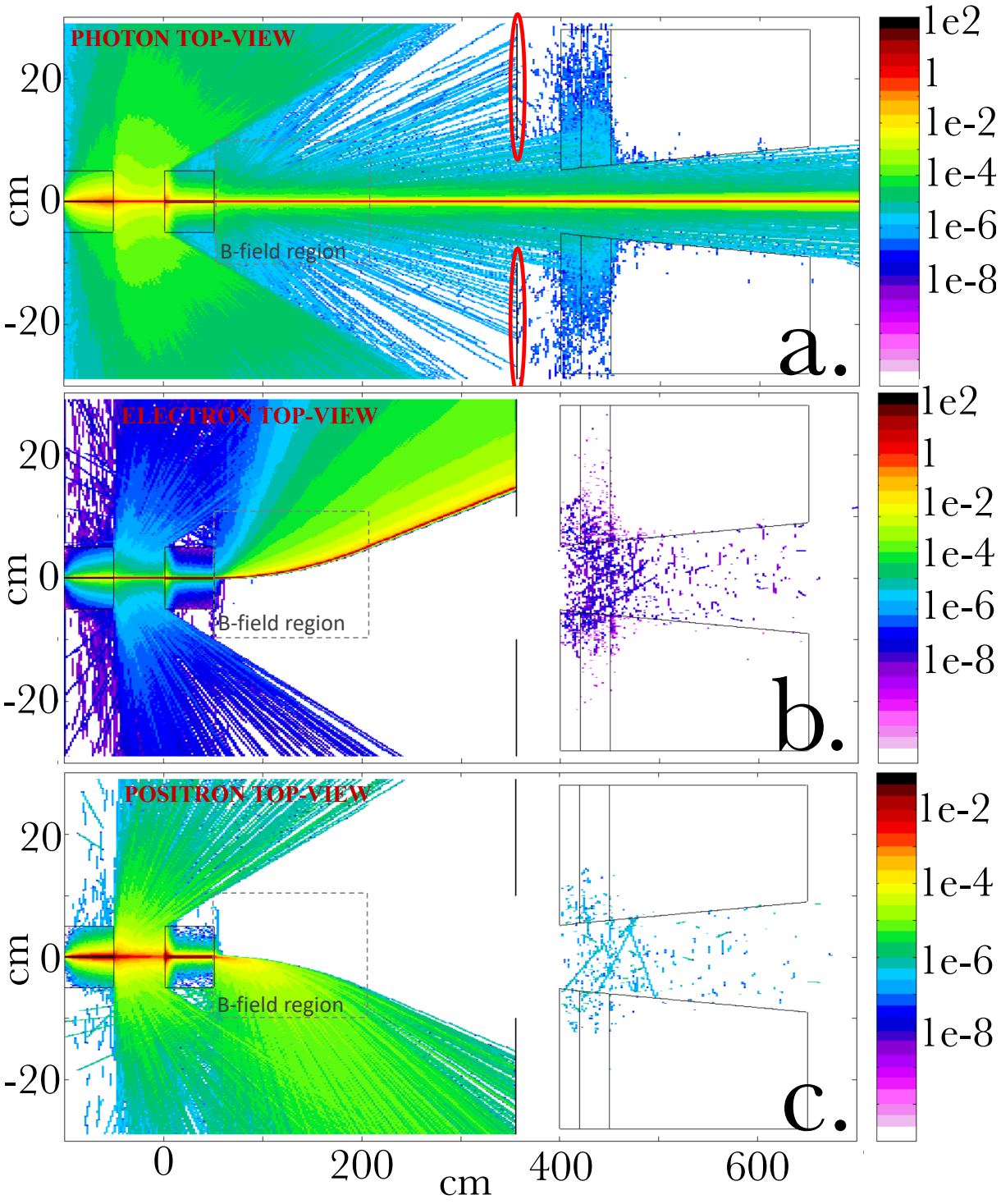

Figure 6: 2-D spatial distribution of photons (a.), electrons (b.), and positrons (c.) for the whole setup. The colour-bars are in number of particles per primary per cm^2, with each spatial bin having an area of 0.25 cm^2. Both spatial axes are in cm. The regions marked with red ellipses in the first frame represent the position of the black-hole total absorbers. Note that the positron graph has a different colour-bar.